BES Analysis Memo

Observation of a near-threshold enhancement in the $p\overline{p}$ spectrum in $J/\psi \to \gamma p\overline{p}$ decays

Stephen L. Olsen

(January 28, 2003)

Abstract

We report the observation of a narrow enhancement near $2m_p$ in the $p\overline{p}$ mass spectrum produced in the radiative decay process $J/\psi \to \gamma p\overline{p}$. The results are based on a 17.8 pb^{-1} data sample that contains 58 million J/ψ decays.

I. INTRODUCTION

In this memo, we report additional supporting material for the proposed paper on the observation of a narrow, resonance-like structure with mass near $2m_p$ in the $p\overline{p}$ system produced in the radiative decay process $J/\psi \to \gamma p\overline{p}$. Earlier versions of this analysis were described in memos posted in March, September and October 2001, and January 2002. This note supersedes some, but not all, of the material in these reports. This memo differs from earlier ones in that the analysis is based on distributions of $M_{p\overline{p}} - 2m_p$, rather than just $M_{p\overline{p}}$. This change eliminates a problem with the bin closest to threshold and causes significant changes in the results for fitting with a resonance shape.

The analysis is based on the entire BES-II 58 million J/ψ event sample. As a calibration process, we have previously identified the process $J/\psi \to \gamma\eta_C$; $\eta_C \to p\overline{p}$. We also have reported results of a search for this state in the BES-I sample of 4×10^6 $\psi(2S)$ events. The absence of any evidence for this state in the $\psi(2S)$ sample provides evidence that the state is produced in J/ψ decays and not in a radiative return process. These results are described in earlier memos as well as in slides from various BES meeting talks that are available on the web [1], and are not repeated here.

II. EVENT SELECTION

We use events with at least two oppositely charged tracks and at least one neutral track with $E_{BSC} > 0.05$ GeV, all in the polar angle region $|\cos\theta| < 0.8$. We assign the highest momentum positively (negatively) charged track as the proton (antiproton) candidate and veto events where *both* candidate tracks are identified as muons or where *both* tracks have associated BSC showers with $E > 0.8$ GeV. Each of the charged tracks is required to have a

dE/dx-derived proton probability greater than that for pions or kaons. Neutral and charged track parameters are corrected with NCOR.F and SUPERFUG.F.

The surviving events are subjected to 4-C fits to the hypotheses $J/\psi \to K^+K^-\gamma$ and $J/\psi \to p\overline{p}\gamma$. If there are more than one candidate γ, the γ that produces the lowest χ^2 to the $J/\psi \to p\overline{p}\gamma$ hypothesis is selected. We select events with a $p\overline{p}\gamma$ fit confidence level greater than 0.05 and greater than that for $K^+K^-\gamma$. From the measured momenta of the candidate p and $\overline{p}$ tracks and the γ direction, we form the quantities $\vec{P}_{\rm miss} = -(\vec{p}_p + \vec{p}_{\overline{p}})$, $E_{\rm miss} = \sqrt{s} - E_p - E_{\overline{p}}$, and $P^2_{\rm tr} = 4P^2_{\rm miss}\sin^2\theta/2$, where $\vec{p}_p$ ($\vec{p}_{\overline{p}}$) denotes the measured momentum and E_p ($E_{\overline{p}}$) the energy inferred for the proton (antiproton) candidate, and θ is the angle between $\vec{P}_{\rm miss}$ and the direction of the candidate γ. We require $|(E_{\rm miss} - |P_{\rm miss}|c)| < 0.1$ GeV and $P^2_{\rm tr} < 0.002$ GeV$/c^2$.

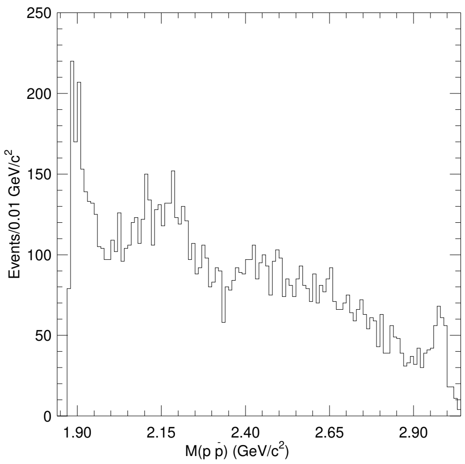

FIG. 1. The $p\overline{p}$ invariant mass distribution from a sample of $J/\psi \to \gamma p\overline{p}$-enriched decays.

Figure 1 shows the $p\overline{p}$ invariant mass distribution for the remaining events. This distribution has a very distinct η_c peak, a broad structure near $M(p\overline{p}) \simeq 2.2$ GeV, and a large narrow peak at the $p\overline{p}$ mass threshold. This latter peak is the subject of this analysis. The $J/\psi \to \gamma\eta_c$; $\eta_c \to p\overline{p}$ channel is studied by the BES-II η_c group [2].

III. THE STRUCTURE NEAR THE $p\overline{p}$ MASS THRESHOLD

A. Is the signal real?

We did some simple checks to demonstrate that the low-mass $p\overline{p}$ peak is not an instrumental effect. Figures 2(a) through (f) show various distributions for events with $M_{p\overline{p}} < 1.9$ GeV.

1. Is some other process fooling the 4-C fit?

Figure 2(a) shows the distribution of $CL(\gamma p\overline{p})$, the 4-C fit confidence level for these events with the $CL > 0.05$ requirement relaxed. Aside from the first few bins, most of which is eliminated by the CL cut, this distribution looks reasonably flat. Figure 2(b) shows the distribution for the proton particle identification probabilities for the tracks in these

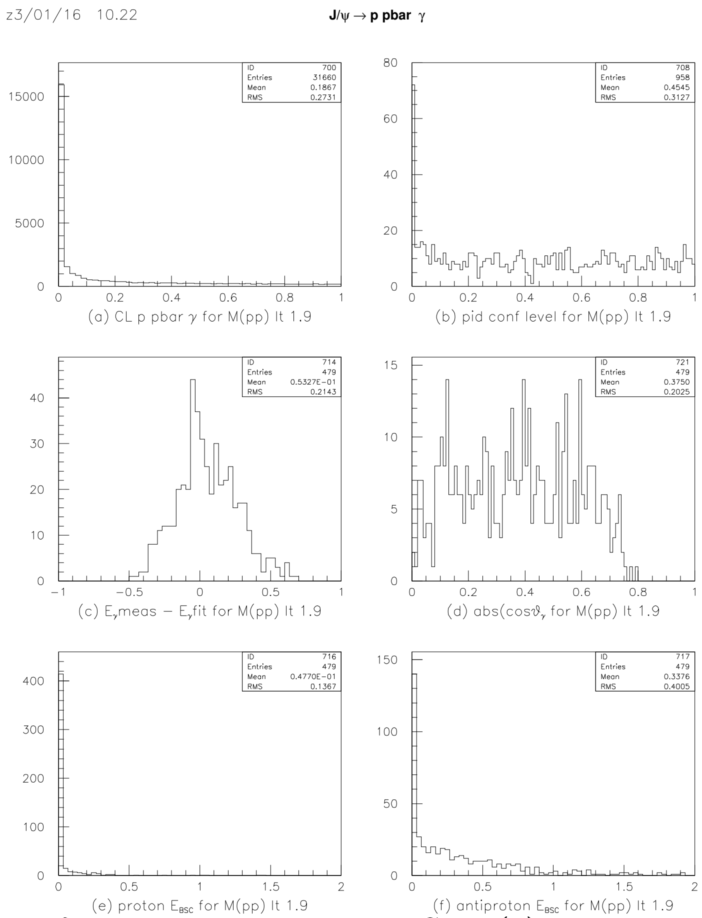

FIG. 2. Distributions for events with $M_{p\overline{p}} < 1.90$ GeV: **(a)** the $\gamma p\overline{p}$ confidence level with the requirement $CL(\gamma p\overline{p}) > 0.05$ relaxed; **(b)** the p and $\overline{p}$ pid confidence level with the pid requirements relaxed; **(c)** difference between measured and fitted γ energies; **(d)** the measured $|\cos\theta_\gamma|$ values; **(e)** the BSC energies for the proton; and **(f)** the BSC energies for the antiproton.

events. These distributions are also reasonably flat and show no peculiar behavior. The pid distributions for tagged samples protons and antiprotons are shown in Fig. 4(a) and (b), which verify that these distributions are as expected.

2. Are the $P^2_{\rm tr}$ or $|(E_{\rm miss} - |P_{\rm miss}|c)|$ requirements doing anything strange?

The $P^2_{\rm tr} < 0.002$ and $|(E_{\rm miss} - |P_{\rm miss}|c)| < 0.1$ requirements, insisted on by some IHEP people, are somehow redundant to a subset of the requirements on the confidence level of the 4-C kinematic fit and, thus, might introduce a bias. The distributions for each of these variables for events with $M_{p\overline{p}} < 1.90$ GeV/c^2 that pass all other requirements are shown in Figs. 3(a) and (b). It is apparent from the figures that the $P^2_{\rm tr} < 0.002$ (GeV/c)^2 and $|(E_{\rm miss} - |P_{\rm miss}|c)| < 0.1$ GeV requirements have no effect on events in this region.

As a result of this, I removed the discussion of the $P^2_{\rm tr}$ and $|(E_{\rm miss} - |P_{\rm miss}|c)| < 0.1$ requirements from the paper draft.

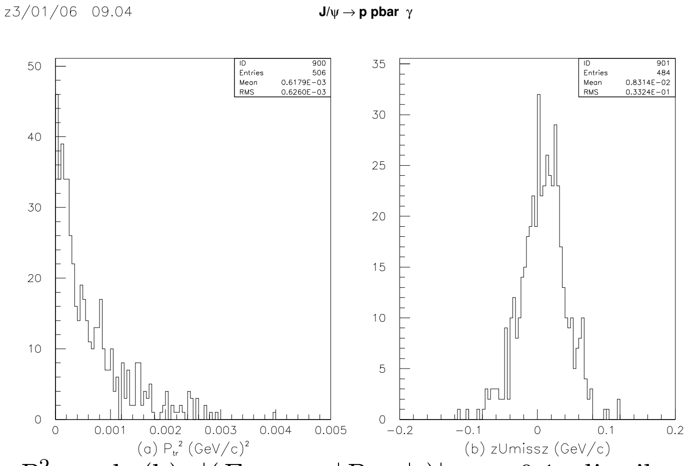

FIG. 3. The (a) $P_{\rm tr}^2$ and (b) $|(E_{\rm miss} - |P_{\rm miss}|c)| < 0.1$ distributions for events with $M_{p\overline{p}} < 1.90$ GeV/c^2 that pass all other $J/\psi \to \gamma p\overline{p}$ selection requirements.

3. Is the peak due to a QED-type background?

One concern is that the peak we see is somehow manufactured by a QED process such as $e^+e^- \to \gamma\gamma$ where one γ converts in the beam pipe and somehow fools the pid and 4-C fit. In this case, the input γ energy would be $E_\gamma = 1.548$ GeV, which is subsequently pulled down by the fit to $E_\gamma \simeq 1.0$ GeV. Figure 2(c) shows the distribution of $E_\gamma^{measured} - E_\gamma^{fitted}$ for selected events. Here it can be seen that the measured energies are rather symmetrically distributed around $E_\gamma \simeq 1.0$ GeV with an rms spread of ~ 210 MeV, as expected for the BSC. There is no evidence for a skewing of energy values on a scale of ~ 0.5 GeV, as would be required for backgrounds that originate from the $e^+e^- \to \gamma\gamma$ process.

Another possible background might be some type of initial-state radiation process. In this case, it would be expected that the γ directions would be concentrated near the beam directions. Figure 2(d)) shows the $|\cos\theta_\gamma|$ distribution for selected events. This distribution shows no strong preference for forward and backward angles. Further evidence against ISR processes is provided by the absence of any evidence for this state in the BES-I $\psi(2S)$ data, as discussed in an earlier analysis memo [3].

4. Are these really protons and antiprotons?

The protons and antiprotons for the $M_{p\overline{p}} < 1.90$ GeV mass range have momenta around 0.5 GeV/c and range out in the TOF scintillators and do not enter the BSC. The BSC energy distribution for the protons, Fig. 2(e), shows this quite clearly. The BSC response for the stopped antiprotons, shown in Fig. 2(f), is quite different, because annihilation products can deposit energy in the BSC.

This characteristic BSC response is demonstrated in Figures 4 (c) and (d), which show the BSC using tagged samples of protons and antiprotons with momenta in in the range $0.4 \le p_{\rm lab} \le 0.6$ GeV/c, respectively. These are selected from a clean sample of $J/\psi \to \Xi^-\Xi^+$ decays, where $\Xi^- \to \Lambda\pi^-$, $\Lambda \to p\pi^-$ and $\Xi^+ \to \overline{\Lambda}\pi^+$, $\overline{\Lambda} \to \overline{p}\pi^+$. The BSC response to K^+ and K^- mesons in a similar range selected from $J/\psi \to K^{*\pm}K^{\mp}$ decays and tagged π^+ and

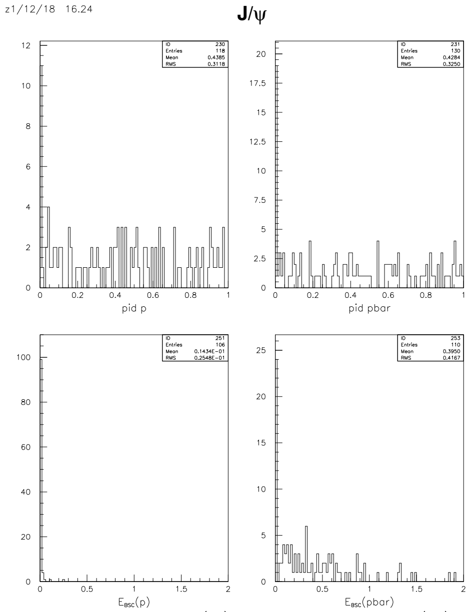

FIG. 4. The pid probabilities for tagged (a) protons and (b) antiprotons in the momentum range $0.4 \leq |\vec{p}| \leq 0.6$ GeV/c from $J/\psi \to \Xi^-\Xi^+$, $\Xi^- \to \Lambda\pi^-$, $\Lambda \to p\pi^-$ (and c.c.) decays. The BSC energy distributions for the same protons (c) and antiprotons (d).

π^- from $J/\psi \to \rho\pi$ decays (not shown) show similar BSC responses positive and negative tracks.

B. Background studies

In order to understand the background, we used SOBER to simulate various J/ψ decay processes that produce final states with $p\overline{p}$ pairs. The simulated events are subjected to the same selection and kinematic fitting criteria as are applied to the data. The results of the study are summarized in Table I, where we list the total number of events that are expected in the 58M J/ψ event sample for each decay mode, using PDG branching fractions, together with the numbers of events that were generated, selected, passed all the cuts and have $M_{p\overline{p}} \leq 1.90$ GeV/c^2. In all cases, phase-space distributions were used. We find that $J/\psi \to \pi^0 p\overline{p}$ is by far the dominant contributor to the background.

To study this background with data we selected events with at least two tracks and two γs that satisfied a 4-C fit to the process $J/\psi \to \gamma\gamma p\overline{p}$ and where the fitted $\gamma\gamma$ invariant mass is within ± 35 MeV/c^2 of m_{π^0} to see if there is any similar structure. The distribution of $M_{p\overline{p}} - 2m_p$ values for $p\overline{p}$ pairs recoiling from the π^0 for these events, shown in Fig. 5(a), shows no prominent feature at low $p\overline{p}$ masses. This distribution is reasonably well represented by a background function of the form $f_{\rm bkg}(\delta) = N(\delta^{1/2} + a_1\delta^{3/2} + a_2\delta^{5/2})$, where $\delta = M_{p\overline{p}} - 2m_p$, and a_1 and a_2 are shape parameters with values determined from the $\pi^0 p\overline{p}$ phase-space MC sample.

We generated a sample of MC simulated $J/\psi \to \pi^0 p\overline{p}$ events with a three-body phase space distribution using SIMBES. We studied how the $\pi^0 p\overline{p}$ feed-down effects the $\gamma p\overline{p}$ sample by subjecting these MC events to the $\gamma p\overline{p}$ selection procedure. Figure 5(b) shows the resulting

TABLE I. Summary of MC background studies

Channel	$N_{expt'd}$	N_{gen}	N_{sel}	N_{cuts}	$N_{Mp\overline{p}<1.9}$
$\pi^0 p\overline{p}$	64K	80K	25.8K	4.5K	27
$\pi^0\pi^0 p\overline{p}$	≤175K	80K	1.9K	11	0
$\eta p\overline{p}$	120K	40K	568	1	0
$\pi^0\Lambda\overline{\Lambda}$	6K	20K	125	7	0
$\pi^+\pi^-\pi^0 p\overline{p}$	135K	40K	33	1	0
$\Sigma^0\overline{\Sigma^0}$	30K	20K	6	0	0
$\pi^+\pi^- p\overline{p}$	350K	40K	11	3	0
$\Lambda\overline{\Lambda}$	35K	20K	3	0	0

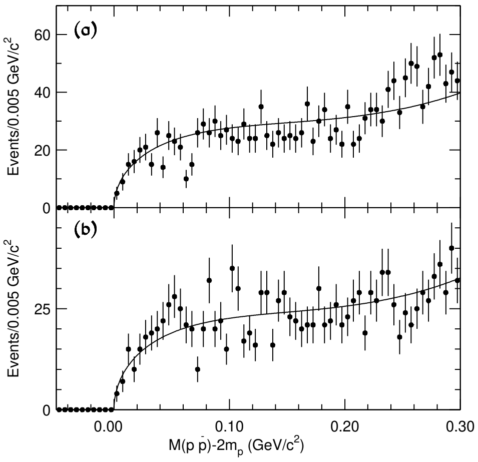

FIG. 5. (a) The distribution of $M_{p\overline{p}} - 2m_p$ values for $p\overline{p}$ pairs recoiling against a π^0 in selected $J/\psi \to \pi^0 p\overline{p}$ events from (a) the data. (b) The corresponding distribution for the $J/\psi \to \pi^0 p\overline{p}$ MC events that pass the $\gamma p\overline{p}$ requirements. The fits are described in the text.

$M_{p\overline{p}} - 2m_p$ distribution. The smooth curve is the result of a fit using the f_{bkg} with shape fixed from the fit to the MC three-body phase space $\pi^0 p\overline{p}$ events. The normalization of this fit relative to that for the $\pi^0 p\overline{p}$-selected MC events is 0.41 ± 0.02 (statistical errors only). The same shape that gives a good representation of the MC phase-space $\pi^0 p\overline{p}$ sample reproduces the features of the $p\overline{p}$ mass spectrum for the $\pi^0 p\overline{p} \to \gamma p\overline{p}$ feed-down events. There is no artificially induced peaking in the low $p\overline{p}$ invariant mass region.

C. Acceptance

The proton and antiproton detection efficiency of the BES detector falls sharply for particles with three-momenta below 0.4 GeV/c. This produces a mass dependence in the experimental acceptance near $M_{p\overline{p}} \simeq 2m_p$ for $J/\psi \to \gamma p\overline{p}$ and $\pi^0 p\overline{p}$. For both processes, when $M_{p\overline{p}}$ is very near $2m_p$, the p and $\overline{p}$ both have three-momenta very near 0.5 GeV/c and are well detected. For increasing $p\overline{p}$ masses, more asymmetric energy sharing is possible and the acceptance decreases until $M_{p\overline{p}} - 2m_p \simeq 2.0$ GeV/c^2, where it is $\simeq 0.67$ of its value at $M_{p\overline{p}} = 2m_p$. This is shown in Fig. 6, where the data points are acceptance values for each mass bin as determined from MC simulations based on SIMBES, with both the γ polar angle distributions and the proton decay angular distribution are generated uniformly. The dashed lines are a fit of two straight lines to the measured acceptance values.

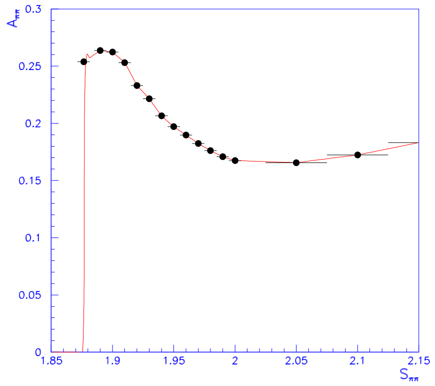

FIG. 6. The variation of the acceptance with $p\overline{p}$ invariant mass for $J/\psi \to \gamma p\overline{p}$ events determined from MC studies using SIMBES.

D. Fitting the near-threshold $p\overline{p}$ mass spectrum

Figure 7(a) shows the near-threshold $M_{p\overline{p}} - 2mp$ distribution for $p\overline{p}$ pairs from the $J/\psi \to \gamma p\overline{p}$-enriched event sample. The acceptance variation is indicated by the dashed curve. We perform a binned, maximum-likelihood fit to this distribution with an acceptance-weighted, modified S-wave Breit Wigner function to represent the signal. We use the form

The S-wave Breit-Wigner formula for a resonance with mass M_0 and width Γ_0 that we use for fitting is

$$f_{BW} \propto \frac{M_0\Gamma_0(q/q_0)k^3}{(M^2 - M_0^2)^2 + (M_0\Gamma_0)^2}, \tag{1}$$

where q_0 (q) is the momentum of a daughter particle for the case where the mass value is M_0 (M) and k is the momentum of the photon, which modifies the BW according to expectations for the $M1$ $1^{--} \to \gamma 0^{-+}$ transition. We represent the background by f_{bkg} with shape parameters fixed from the fit to the $p\overline{p}$ masses for the $\pi^0 p\overline{p}$ data sample shown above in Fig. 5(a). The fit, shown as the solid curve in Fig. 7, has $\chi^2/d.o.f. = 56.3/56$, which corresponds to a confidence level of 46.2%.

The results of the fit for the signal Breit Wigner function are: $N_{evts} = 928 \pm 57$, $M = 1859 \pm 3$ MeV/c^2 , and $\Gamma = 0.0 \pm 21$ MeV/c^2, where only statistical errors are listed. The fitted f_{bkg} component, shown in the figure as a dotted line, has a normalization that is 0.86 ± 0.06 times that for the fit to the $\pi^0 p\overline{p}$ sample. This is about twice the MC expectation for feed down from from the π^0 channel (0.41 ± 0.02) and indicates that about half of the background is due to non-resonant $J/\psi \to \gamma p\overline{p}$ decays.

The below-threshold mass and narrow width are very suggestive of a bound $p\overline{p}$ state. In Fig. 7(b), we show the $M_{p\overline{p}} - 2mp$ distribution where each event is weighted by a factor of

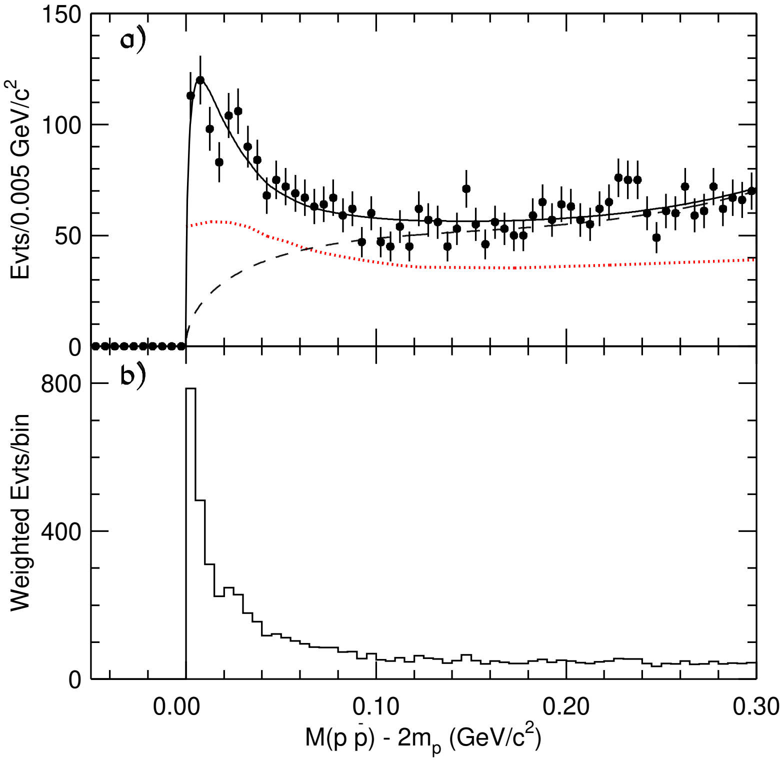

FIG. 7. (a) The fit to $M_{p\overline{p}} - 2m_p$ distribution for $p\overline{p}$ pairs in the $J/\psi \to \gamma p\overline{p}$-enriched event sample with an acceptance-weighted S-wave Breit Wigner function used to represent the signal. The solid curve is the result of the fit, the dashed curve is the background component and the dotted curve indicates the acceptance variation as a function of $M_{p\overline{p}}$. (b) The $M_{p\overline{p}} - 2m_p$ distribution of events weighted by q_0/q.

q_0/q, where we use $q_0 = 0.35$ GeV/c, corresponding to $M_{p\overline{p}} = 2$ GeV. The sharp upturn in the bin closest to threshold is as expected for an S-wave BW with peak mass below threshold.

I also tried fits using P-wave and D-wave Breit-Wigner functions to represent the data. The P-wave BW fit has $\chi^2/d.o.f. = 59.0/56$, worse than the S-wave fit, but still acceptable. In this case the peak mass is very nearly equal to $2m_p$, i.e. $M = 1876.4 \pm 0.9$ MeV$/c^2$, and the total width is quite narrow: $\Gamma = 4.6 \pm 1.8$ MeVc^2. The fit with a D-wave BW fails badly; in this case $\chi^2/d.o.f. = 1405/56$.

1. *Other fits*

We also fit the near threshold $p\overline{p}$ mass spectrum for the $\gamma p\overline{p}$-enhanced event sample with f_{bkg} only. Figure 8(a) shows the result of a binned likelihood fit using f_{bkg} alone, with the normalization (A_0) and both shape parameters (A_1 and A_2) allowed to float. This fit does not provide an acceptable representation to the data. Figure 8(b) shows the result of a fit with the background shape parameters free to vary. This fit gives the same mass and width as the fit with A_1 and A_2 fixed at the three-body phase space values, but a signal yield of 1022 ± 128 events, which is 10% higher than the best fit value. This type of variation is discussed below in the section on systematic errors.

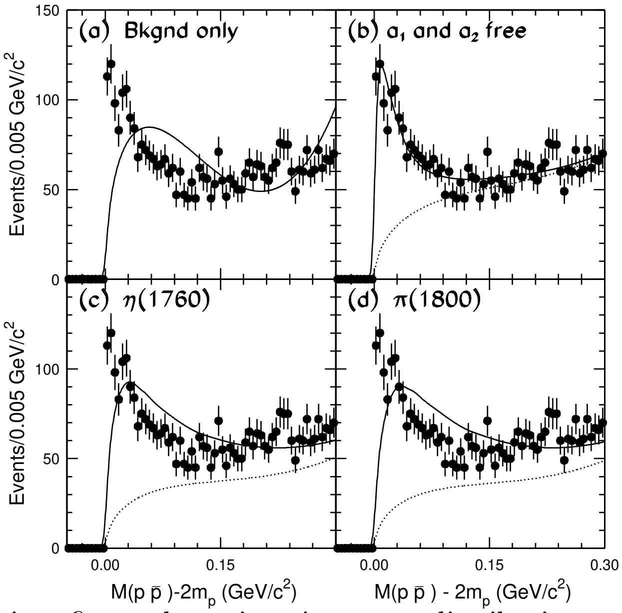

FIG. 8. Results of various fits to the $p\overline{p}$ invariant mass distribution near the $p\overline{p}$ mass threshold. The fits include: (a) background only with shape parameters free; (b) signal with shape parameters free to float; (c) an S-wave Breit-Wigner function with mass and width from the $\eta(1760)$ plus a background with the $p\overline{p}\pi^0$ shape; and (d) same as (c) but with the BW mass and width fixed at the PDG values for the $\pi(1800)$.

We tried to fit the data with known particle resonances to represent the low-mass peak. Since the peak is very close to threshold, we restrict ourselves to the case where the p and $\overline{p}$ are in an S-wave. Since, as discussed above, we rule out the possibility of this state being produced by a radiative return process, the S wave assumption implies a $J^{PC} = 0^{-+}$ pseudoscalar state. There are two pseudoscalar resonances listed in the PDG tables [4] in this mass region: the $\eta(1760)$ with $M_{\eta(1760)} = 1.760 \pm 0.011$ GeV and $\Gamma_{\eta(1760)} = 0.060 \pm 0.016$ GeV, and the $\pi(1800)$ with $M_{\pi(1800)} = 1.801 \pm 0.013$ GeV and $\Gamma_{\pi(1800)} = 0.210 \pm 0.015$ GeV. Figure 8(c) shows the result of a fit with a background function with shape fixed from the $p\overline{p}\pi^0$ fit and an S-wave Breit-Wigner function with mass and width fixed at the PDG values for the $\eta(1760)$. This fit has $\chi^2/n_{dof} = 323.4/58$. A fit with the $\pi(1800)$ parameters, shown in Fig. 8(d). is somewhat worse with $\chi^2/n_{dof} = 411.8/58$.

E. Angular distributions

For a pseudoscalar $p\overline{p}$ state, the photon polar angle, θ_γ, is expected to have a $1 + \cos^2\theta_\gamma$ distribution. Figure 9(a) shows the $|\cos\theta_\gamma|$ distribution for events with $p\overline{p}$ mass below 1.90 GeV; Fig. 9(b) shows the same distribution for the selected $\pi^0 p\overline{p}$ events, also with $p\overline{p}$ masses below 1.90 GeV. For these plots, the vertical scale is numbers of events per bin. Figure 9(c) shows the background-subtracted and acceptance corrected distribution together with a fitted curve of the form $1 + \cos^2\theta_\gamma$ for $|\cos\theta_\gamma| < 0.8$. Here, "background subtracted" means we subtract the $\pi^0 p\overline{p}$ data distribution (Fig. 9(b)) from the $\gamma p\overline{p}$ distribution (Fig. 9(a)) after normalizing to the background fraction of events below $M = 1.90$ GeV from the fit (the normalization factor is nearly 1), and acceptance corrected means dividing by the SIMBES MC distribution, shown in Fig. 9(d). The vertical scale of Fig. 9(c) is $dN/d|\cos\theta_\gamma|$.

The fit for $1+\cos^2\theta_\gamma$ to the $|\cos\theta_\gamma| < 0.8$ region has $\chi^2/d.o.f. = 3.7/7$. For comparison, a fit to $\sin^2\theta_\gamma$, shown as the dashed line, has $\chi^2/d.o.f. = 10.3/7$. Although both fits are acceptable, the $1+\cos^2\theta_\gamma$ form expected for a pseudoscalar state is preferred

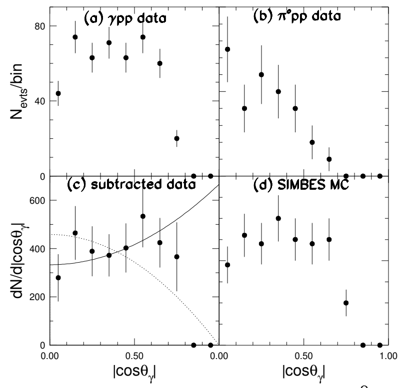

FIG. 9. The $|\cos\theta_\gamma|$ distribution for the (a) $\gamma p\overline{p}$ and (b) $\pi^0 p\overline{p}$ data samples for $M_{p\overline{p}} < 1.9$ GeV. (c) The background-subtracted, acceptance-corrected distribution The solid curve is a fit for $1+\cos^2\theta_\gamma$ to the $|\cos\theta_\gamma| < 0.8$ region; the dashed curve is a fit for $\sin^2\theta_\gamma$. (d) The $|\cos\theta_\gamma|$ distribution for SIMBES-generated $\gamma p\overline{p}$ events.

F. Measurement biasses

Since the peak mass is below the threshold, we are attempting to determine the mass and width of the BW from the tail. This may result in biased measurements. We tested for biases in the analysis using samples SIMBES-generated events with S-wave BW shapes with different masses and widths. The same analysis applied to these events finds output values close to the MC inputs (see Table II). We conclude that in the absence of background bias on the mass is negligible compared to other systematic errors, and on the width is small.

TABLE II. Results of the S-wave Breit Wigner Monte Carlo simulations for different generated masses and widths.

M_{in} (MeV/c^2)	Γ_{in} (MeV/c^2)	M_{out} (MeV/c^2)	Γ_{out} (MeV/c^2)
1860	20	1860 ± 2	28 ± 4
1860	50	1861 ± 2	57 ± 3
1870	20	1869 ± 1	21 ± 1
1870	50	1869 ± 2	53 ± 1
1880	20	1880 ± 1	22 ± 1
1880	50	1881 ± 1	53 ± 1
differences		+1 -1	+7 -0

However, biasses can occur in the presence of background. To test eight event samples were generated for each of three cases: $M = 1860$, $\Gamma = 20$ MeV/c^2, $M = 1860$, $\Gamma =$

2 MeV/c^2, and M = 1850, Γ = 10 MeV/c^2 (24 samples in total). These samples include background at the experimentally observed level. Figure 10 shows the difference between the fitted mass and the input value. The difference values cover the range $-2 \leq (M_{fit} - M_{in}) \leq$ 24 MeV/c^2, with an overall positive bias that indicates a fitted mass that tends to be larger than the input mass on average by about 20 MeV/c^2.

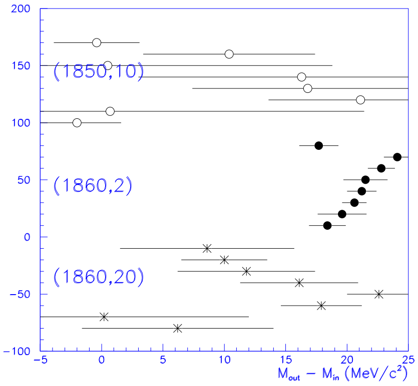

FIG. 10. Differences between fitted and input mass for different SIMBES event samples.

Figure 11 shows the corresponding plot for the differences between the fitted and input width values. Here there is some scatter and the difference values cover the range $-10 \leq (\Gamma_{fit} - \Gamma_{in}) \leq 42$ MeV/c^2, with an overall positive bias that makes the fitted mass on average about 15 MeV/c^2 larger than the input value.

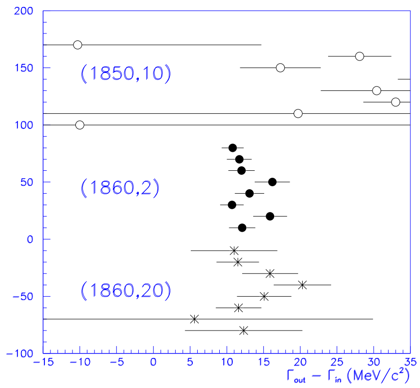

FIG. 11. Differences between fitted and input width for different SIMBES event samples.

G. Systematic errors

To determine the systematic errors associated with uncertainties in the fitting procedures, we did the signal fits different ways and recorded the differences. The results are summarized in Table III. These include changes in the background shape parameters, resolution values, bin sizes and acceptance. I also made a rough test of the sensitivity of my fits to possible effects of a broad resonance around 2.2 GeV, by including a standard BW function with M fixed at 2.2 GeV and Γ fixed at 0.2 GeV and 0.3 GeV. Here, the entries in the "quadrature sums" row of Table III correspond the the quadrature sum of the extreme entries for background variations, resolution, Sober *vs* SIMBES, bin size, BW tests, and using a χ^2 fit rather than Likelihood.

TABLE III. Changes in the number of signal events, δN_{evts}, the peak mass, δM, and peak width, $\delta\Gamma$, for different variations of the fit as explained in the text.

Fit variation	$\delta(in\%)$	δM (MeV/c^2)	$\delta\Gamma$ (MeV/c^2)
A_1 & A_2 at $\pi^0 p\overline{p}$ values	+202	-7	0
Float A_1 & A_2	+94	-2	0
resolution$\sigma = 1$ MeV	0.0	+1	0
resolution$\sigma = 3$ MeV	+3	+3	0
resolution$\sigma = 6$ MeV	+27	+5	0
SOBER acceptance	+84	0	0
Coarser bins	+11	-2	0
BW at 2.2 GeV ($\Gamma = 0.2$ GeV)	+17	0	0
BW at 2.2 GeV ($\Gamma = 0.3$ GeV)	+43	-1	0
Likelihood$\rightarrow \chi^2$	-15	0	0
Quadrature sums	$^{+224}_{-15}$	$^{+5}_{-7}$	$^{+0}_{-0}$

Another systematic error on the branching fraction is the uncertainty in the number of J/ψ events in the data sample (5%).

For the systematic error on the event yield, I combine the quadrature sums from Table III with the 5% uncertainty in the number of J/ψ events and a 10% uncertainty in acceptance to get $^{+27\%}_{-11\%}$. For the mass, I add the Quadrature Sum results from Table III, to the range of differences seen in the bias study to get $^{+5}_{-25}$ MeV. For the width, the corresponding error range is $^{+10}_{-42}$ MeV. for the upper limit, I add the positive systematic error to the statistical error in quadrature and multiply by 1.28 to get 30 MeV as the 90% CL upper limit.

1. Branching fraction determination

Using the MC-determined acceptance of 0.23, this corresponds to a product of branching fractions of:

$$\mathcal{B}(J/\psi \rightarrow \gamma X_{\overline{N}N(1859)})\mathcal{B}(X_{\overline{N}N(1859)} \rightarrow p\overline{p}) = (7.0 \pm 0.4^{+1.9}_{-0.8}) \times 10^{-5}.$$

(Some authors have reported evidence for narrow $\overline{N}N$ states in this mass region [5].)

IV. SUMMARY AND DISCUSSION

We observe an narrow enhancement in the $p\overline{p}$ mass distribution very near the $p\overline{p}$ mass threshold. When treated as a resonance, we determine of $1859 \pm 3^{+5}_{-25}$ MeV/c^2 a narrow width that is narrower than 30 MeV/c^2 at the 90% confidence level. No instrumental or background source for this peak can be found. A similar analysis applied to the same data sample finds a signal for $J/\psi \to \gamma\eta_C$; $\eta_C \to p\overline{p}$ with mass and branching fractions consistent with PDG values. No evidence is found for this structure in the $\psi(2S)$ data sample. This rules out the possibility that the observed state is produced by a radiative return process that is unrelated to J/ψ decays.

The sub-threshold mass and narrow width are strongly suggestive of a $p\overline{p}$ bound state as first proposed by Fermi and Yang [6].

V. ACKNOWLEDGEMENT

I gratefully acknowledge the considerable assistance I received from Xiaobin Ji and many useful comments from Bill Dunwoody.

REFERENCES

[1] Copies of transparancies for BES video meeting presentations and previous analysis memos can be accessed at www.phys.hawaii.edu/ solsen/besec/slo.html.

[2] J.Z. Bai *et al.* (BES-II Collab.) *Measurements of the Mass and Width of the* η_c *Meson*, to be submitted to Physics Letters B.

[3] Analysis memo of January 15, available at www.phys.hawaii.edu/ solsen/besec/slo.html.

[4] D.E. Groom *et al.* (PDG), Eur. Phys. Journ. **C15**, 1 (2000).

[5] See, for example, A. Antonelli *et al.*, Nucl. Phys. **B517**, 3 (1998), G. Bardin *et al.*, Nucl. Phys. **B411**, 3 (1994), and O.D. Dalkarov *et al.*, Phys. Lett. **B392**, 229 (1997).

[6] E. Fermi and C.N. Yang, Phys. Rev. **76**, 1739 (1949). For a recent review of this subject, see J-M. Richard, Nucl. Phys. Proc. Suppl. **86**, 361 (2000).